16th World Conference on Earthquake Engineering, 16WCEE 2017

Santiago Chile, January 9th to 13th 2017

Paper N° 2598

Registration Code: S-D1464734516

SHAKE-TABLE TESTING OF NON-DUCTILE RC FRAMES AS-BUILT AND RETROFITTED WITH GFRP LAMINATES AND SLAB-WEAKENING

P. Quintana Gallo [(1)], S. Pampanin [(2)], A. J. Carr [(3)]

[(1)] Research Structural Engineer, BRANZ, Porirua, Wellington, New Zealand, patricio.quintana-gallo@branz.co.nz
[(2)] Professor, Department of Civil and Natural Resources Engineering, University of Canterbury, Christchurch, New Zealand, stefano.pampanin@canterbury.ac.nz
[(2)] Emeritus Professor, Department of Civil and Natural Resources Engineering, University of Canterbury, Christchurch, New Zealand, athol.carr@canterbury.ac.nz

Abstract

To investigate the response of non-ductile reinforced concrete (RC) frame buildings under earthquake ground motions, before and after retrofit, a series of uni-directional shake-table experiments was carried out at the University of Canterbury. The 2/5 scale, 3-storey, 2-by-1 bay specimen was tested as-built, as-built/repaired, and retrofitted with Glass Fibre Reinforced Polymer (GFRP) laminates and weakening of the floor slabs, following a partial retrofit strategy. The as-built specimen was subjected to a single short duration motion at increasing amplitudes. The as-built/repaired and retrofitted specimens were tested using two different input motions with as-recorded amplitudes only, with relatively short and long durations, respectively. The experimental results showed that the as-built specimen remained essentially elastic during the first test and developed a column lap-splices failure in the top floor during the third and most demanding test. The as-built/repaired specimen experienced very little damage during the first test and severe damage in first floor exterior beam column joints (b-c joints) and interior columns during the second. The retrofitted specimen showed no damage during the first experiment and large flexural cracking in the beams of exterior b-c joints of the first two floors during the second one. This paper briefly presents the features of the experimental model and the developed retrofit solution. It also summarizes some of the results with emphasis on the impact of the input duration on the magnitude of the response and the intensity of the damage experienced by the structure.

Keywords: Shake-Table Testing; Non-Ductile RC Frames; Seismic Assessment; Seismic Retrofit; GFRP laminates

1. Introduction

Experiences with damaging earthquakes as well as research findings have shown the seismic vulnerability of many reinforced concrete (RC) frame buildings designed according to old codes (pre-1970's). These findings have promoted the development and application of several assessment procedures and retrofit strategies. To date, extensive experimental research has been conducted in substandard beam-column joint (b-c joints) subassemblies [1-8] and frame assemblies [9, 10] subjected to quasi-static or pseudo-dynamic (uni- or bi-directional) lateral loading, as-built and in some cases retrofitted. A relatively smaller number of shake-table experiments have been carried out until now [11-18]. Only some of those specimens included the investigation of a new retrofit solution [14-18].

Bracci et al. tested a 1/3 scale, 3-storey model with symmetric 3-bay internal frames designed to resist gravity loads only, as-built [13] and retrofitted with prestressed concrete and masonry block jacketing, and partial masonry infill techniques [14]. Chaudat et al. [15] performed experiments on a full-scale, 2-storey, 1 by 1 bay model, with external frames only. The specimen, which included floor slabs, was tested as-built and retrofitted with Carbon Fibre Reinforced Polymer (CFRP) laminates. A similar specimen was tested by Garcia et al. [16] as-built and retrofitted with post-tensioned metal straps (PTS) [16], and a combination of CFRP and PTS [17]. Sharma et al. [18] tested a planar 2/3 scale 2-storey 1-bay specimen (i.e. without transverse beams and floor slabs), as-built and retrofitted with the haunch retrofit solution [19]. All these experimental models included exterior b-c joints with non-seismic detailing. Some of them included lightly confined exterior b-c joints of internal frames (cruciform). Others had exterior b-c joints of external frames (corner) only with no stirrups in the joint. One, with the most vulnerable reinforcement detailing (similar to the one used of this research), was planar, i.e. it did not include slabs and transverse beams.

In the research presented herein, a 2/5-scale experimental model that included two 3-storey, 2-bay asymmetric frames in parallel, external and internal, joined together by transverse beams and floor slabs, was selected. This resulted in a geometry that allowed the assessment and development of a retrofit solution for corner and cruciform b-c joints with floor slabs at the same time. The specimen was constructed with particularly vulnerable characteristics [4, 6], including smooth bars, no stirrups inside the joint, 180° beam end-hooks, lap-splices in potential plastic hinge regions, and substandard quality materials. It was tested under unidirectional shake-table motion as-built (with lap-splices), as-built/repaired (without lap-splices), and retrofitted with Glass Fibre Reinforced Polymer (GFRP) laminates combined with weakening of the floor slabs.

This paper presents the main characteristics of the experimental model and the most relevant features of the developed retrofit solution. It also shows and compares some of the experimental results with emphasis on the influence of the duration and frequency characteristics of the input motion on the observed response of the specimens. The results confirmed, in the dynamic range, the seismic vulnerability of the structural typology under investigation. They also showed the efficacy of the developed retrofit solution under extremely adverse conditions as a result of an apparent resonance during the long duration tests.

2. Description of the experimental model

2.1 Geometry and reinforcing details

The design of the experimental model was based on the planar prototype frame introduced by others [20]. Two of those frames were scaled down in the linear dimensions by the factor l_r = 2/5 and connected in parallel with scaled down transverse beams and cast-in-situ slabs. On the exterior face of one of the frames, an overhang or stub was used to simulate an internal frame. The resulting specimen is a three-dimensional structure whose size and weight fully exploited the facilities of the structures laboratory of the University of Canterbury. Fig. 1 shows the geometry and the main reinforcing characteristics of the longitudinal frames.

Fig. 1(a) presents a picture of the building taken from the south-east corner. Fig. 1(b) shows the longitudinal elevations of the structure (i.e., of the frames that run in the north-south direction). As shown in these figures, the model had a total height of 3600mm above the footings, with inter-storey heights of 1200 mm. It extended 3000 mm in the longitudinal direction, with long and short spans of 1800mm and 1200 mm, respectively. The frames were spaced at 1200mm in the short direction, with stubs extending 300mm beyond the centreline of the west frame, forming cruciform exterior b-c joints in the north and south facades. All the columns and beams had 140/140mm and 140/200mm (width/height) cross-sections, respectively. The slab was 60mm thick. All the longitudinal reinforcement and stirrups consisted in 6mm bars and 4mm wire, respectively. Fig. 2 shows the reinforcing detailing of corner and cruciform exterior b-c joints. Further details can be found in [21].

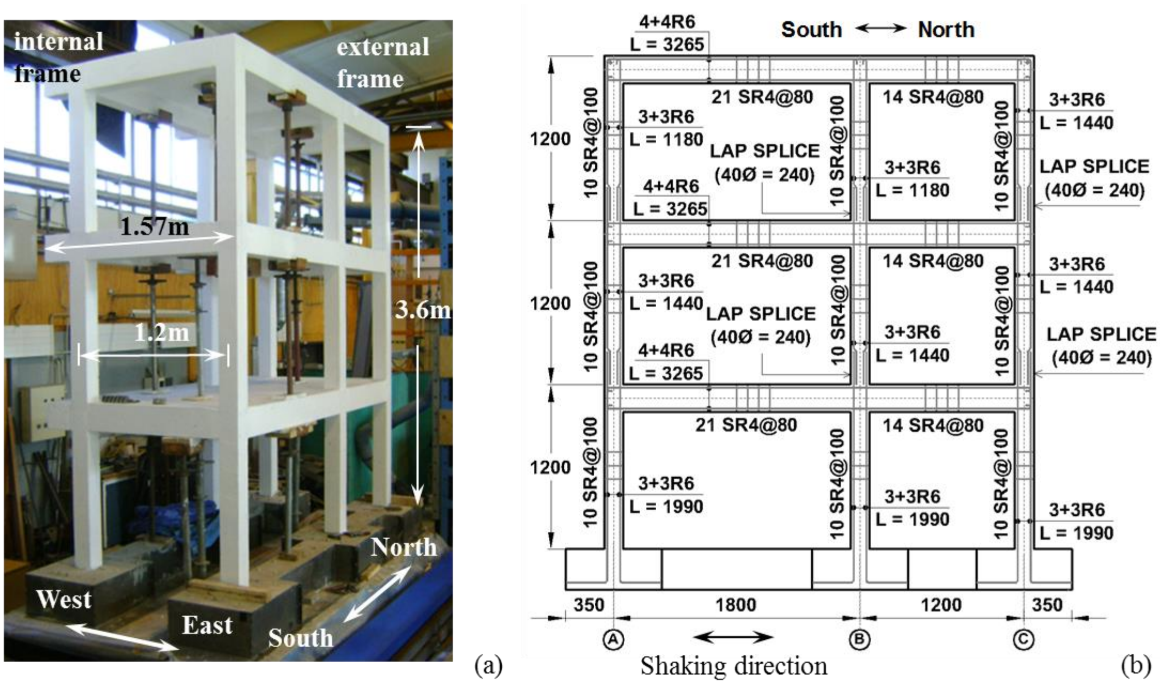

Fig. 1 – (a) Building perspective from the south-east corner; (b) longitudinal frames elevation. Note: all dimensions in mm; shaking direction: south-north.

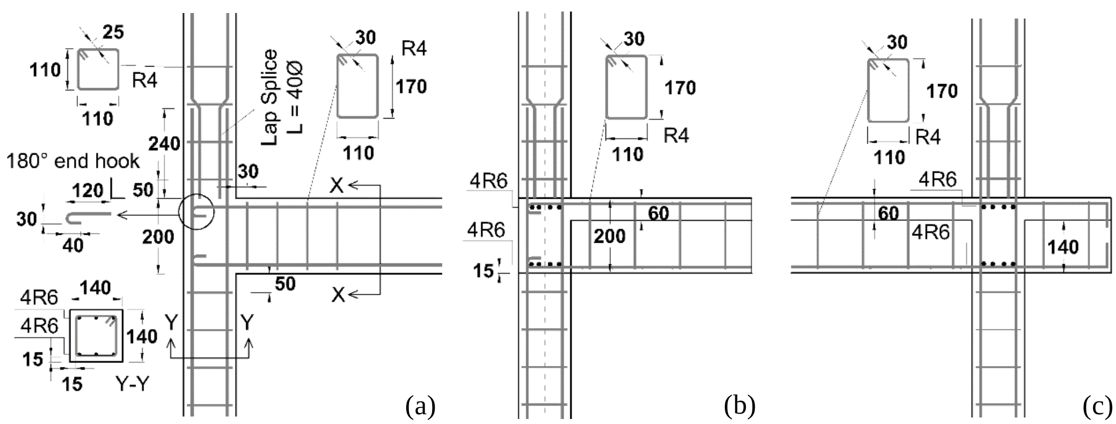

Fig. 2 – (a) Reinforcing details of exterior b-c joints; (b) beam cross-section corner joints; (c) beam cross-section cruciform joints. Note: all dimension in mm.

2.2 Materials

All 6mm bars were made of 300 MPa mild steel (type 1), whereas the 4mm stirrups were made of 500 MPa steel wire (type 2). The average measured yield and ultimate stresses of steel type 1 were 385 MPa and 500 MPa, respectively, with strains at hardening and rupture of approximately 1% and 10%, respectively. The average measured stresses at yielding and rupture of steel type 2 were 550 MPa and 600 MPa, respectively, with a rupture strain of 1.4% (without hardening). The average measured values of the maximum compressive stress of the concrete, f_c', were 30 MPa, 25 MPa and 12 MPa for floors 1, 2 and 3, respectively. The particularly low value of f_c' in the third floor was due to excessive water in the concrete mix, accidentally representative of the poor quality of the materials associated with the building typology under investigation.

2.3 Similitude requirements

The main goal during the design of the specimen was to develop an experimental model able to represent, with the lesser degree of distortion, the dynamic response of the prototype. The main source of distortion was the use of prototype materials, such that the mechanical properties of the steel and concrete were the same in the prototype and model domains [22]. As a result, the density of the model structure should be scaled up by a factor $\rho_r = 1/l_r = 2.5$, which is a very impractical task. Nevertheless, this limitation was overcome by using additional artificial mass at each floor level, evenly distributed in plan, following the method suggested in [23]. In this case, 4.3 tons and 3.0 tons were added to the model in the first two levels and the roof, respectively, in the form of steel plates and concrete blocks. With the additional mass, the total weight of the model was 18.5 tons, approximately.

2.4 Repairing/modification of the as-built specimen

After the first series of experiments was performed, the as-built specimen was modified by connecting the lap splices of all the columns. The procedure included removal of the concrete in the lap-splice area, welding the spliced bars, and encasing with structural mortar (f_c' = 33 MPa) to replace the previously removed concrete [21].

3. Retrofit intervention

The retrofit intervention followed a partial retrofit strategy as defined in [24]. That is, only the exterior b-c joints were upgraded, accepting flexural hinging in the interior columns of both frames. The objective of the retrofit strategy was to reverse the hierarchy of strengths in the exterior b-c joints, forcing the damage to occur in the beams, to impose a more ductile and stable inelastic mechanism in the structure. The retrofit solution consisted of (1) GFRP laminates to strengthen the b-c joints and (2) weakening of the slab to reduce the flexural capacity of the beam under negative bending moments outside the strengthened region. Fig. 3(a) shows a three-dimensional drawing of the retrofitted specimen, Fig. 3(b) to 3(d) present the four b-c joint types upgraded in this case, and Fig. 3(f) and 3(g) present pictures of a retrofitted corner and a cruciform b-c joints, respectively.

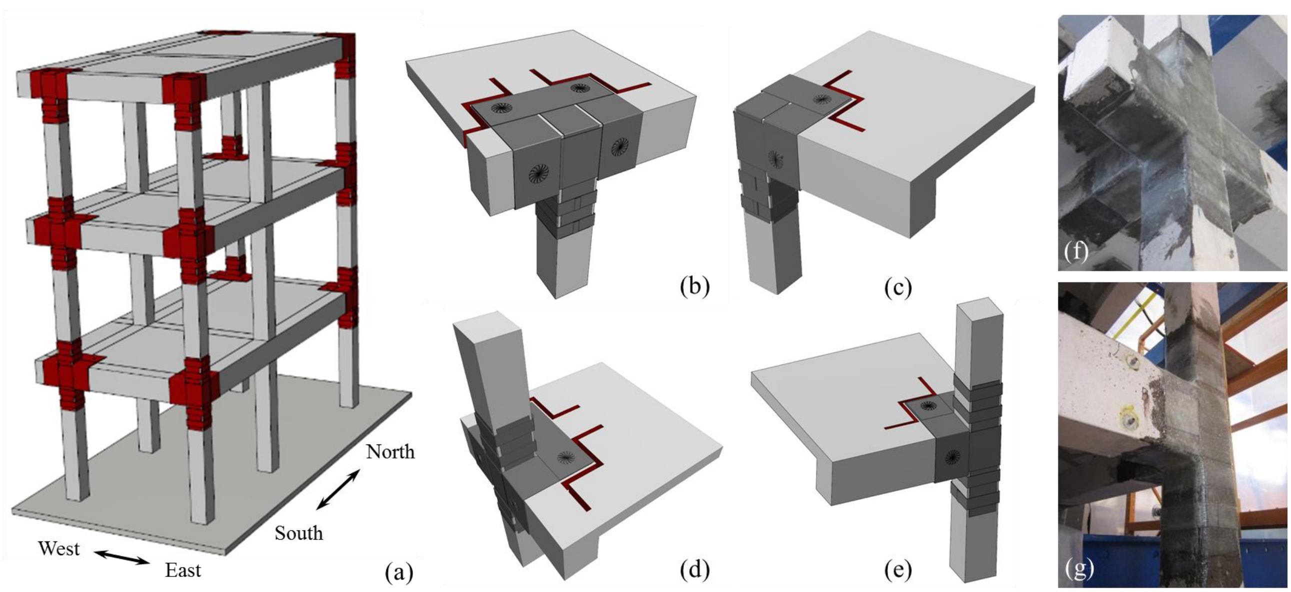

Fig. 3 – Retrofitted: (a) specimen; (b) roof cruciform b-c joint; (c) roof corner b-c joint; (d) typical floor cruciform b-c joint; (e) typical floor corner b-c joint; (f) picture of strengthened cruciform b-c joint; (g) picture of strengthened corner b-c joint.

SikaWrap 100-G, type E-Glass uni-directional GFRP laminates were used for the strengthening solution due to their relatively lower cost and ability to sustain larger strains before rupture when compared to their carbon-based counterparts (CFRP). The mechanical properties of the 0.36 mm thick fabric sheets are: Young's modulus E_f = 76,000 MPa, nominal tensile strength σ_{fu} = 2,300 MPa, and strain at break of fibers ε_{fu} = 2.8%. The layout of the laminates, bonded to the concrete surface, was based on the arrangement previously developed by others for planar and three-dimensional beam column joints without floor slabs [25, 9]. The number and preliminary dimensions of the GFRP layers was calculated following the methodology presented in [26], modified to account for the slab and the transverse beam [21]. The length of the laminates in beams and columns, initially estimated to prevent debonding, was determined using the bending moment diagrams of a static-admissible and kinematic-compatible inelastic mechanism [21]. In addition, some of the sheets were anchored with GFRP dowels to enhance the bond resistance between them and the concrete.

The slab was weakened by saw-cutting its reinforcement (a single mesh in this case) to reduce the flexural strength of the beam under negative bending moments. This allowed the inelastic rotations to take place in the beam cross-sections outside the GFRP-strengthened region, where the fuse was forced to occur. The shape of the weakening gap was defined by accounting for the load path in the slab, and was conceived to be effective also under bi-directional loading, aiming for practical applications.

The retrofit solution was implemented following the steps presented in detail in [21]. Those steps include: (1) bonding of the laminates to the concrete surface, (2) insertion of GFRP dowels in the beams and the slab to provide anchorage, and (3) slab-weakening. Fig. 4 and Fig. 5 show a compact version of the sequence of application of the retrofit solution in corner and cruciform b-c joints of typical storeys, respectively. The implementation of the retrofit solution in roof b-c joints can be found in [21].

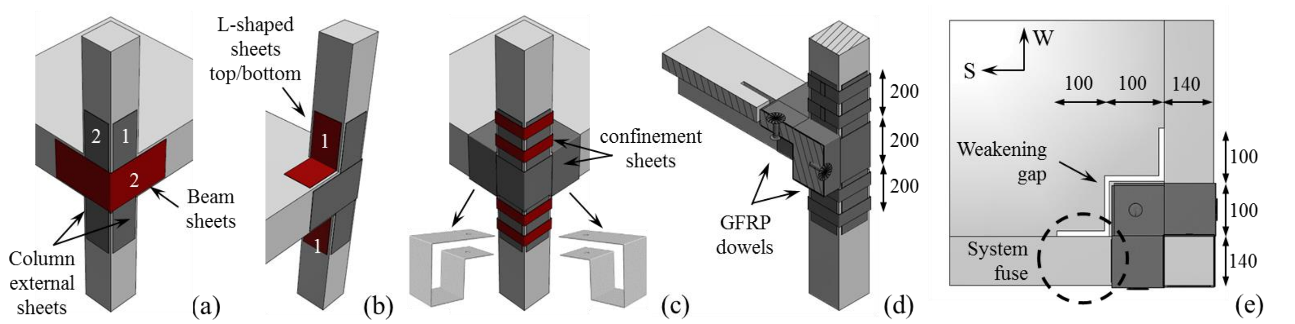

Fig. 4 – Retrofit of corner b-c joints, short span: (a) external column and beam laminates; (b) internal L-shaped column sheets; (c) confinement sheets; (d) anchorage on beam and slab; (e) slab-weakening. Notes: all dimensions in mm; numbers on sheets indicate number of layers; confinement sheets are 1 layer only.

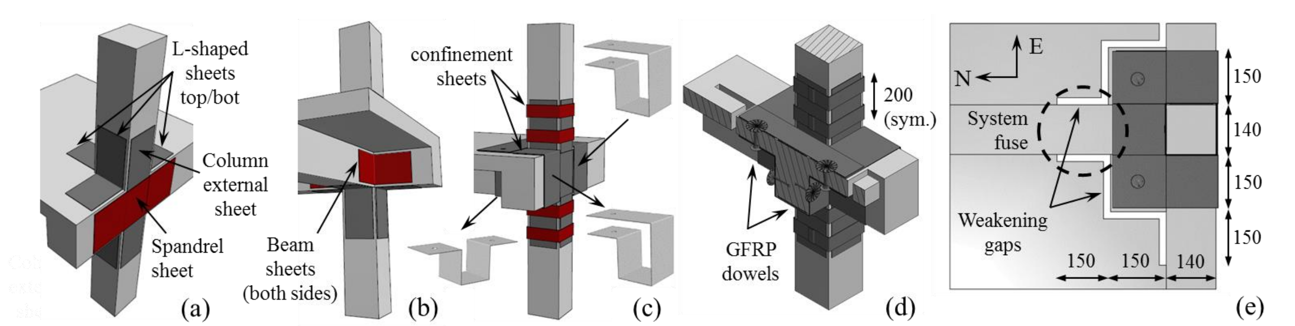

Fig. 5 – Retrofit of cruciform b-c joints, long span: (a) column and spandrel laminates; (b) beam internal laminates; (c) confinement sheets; (d) anchorage on beam and slab; (e) slab-weakening. Notes: dimensions in mm; all sheets are 1 layer only.

4. Testing protocol

The entire experimental campaign comprised three series of uni-directional shake-table tests: (1) S1: as-built specimen, with column lap-splices, (2) S2: as-built/repaired specimen after welding the lap-splices, and (3) S3: retrofitted specimen. In series S1, a single input motion (GA7) at three increasing amplitudes was used. In series S2 and S3, two records (CCH and VMM) were used, each of them during one test only. Fig. 6 shows the acceleration input motions and their elastic displacement response spectra at 5% critical damping ratio (ξ). Table 1 presents information relative to the earthquake ground motions, including epicentre-to-station distance (R), significant duration (D_s) [27], and the peak ground acceleration (PGA). Table 2 presents the experimental matrix of the tests included in this paper, with their respective input motions.

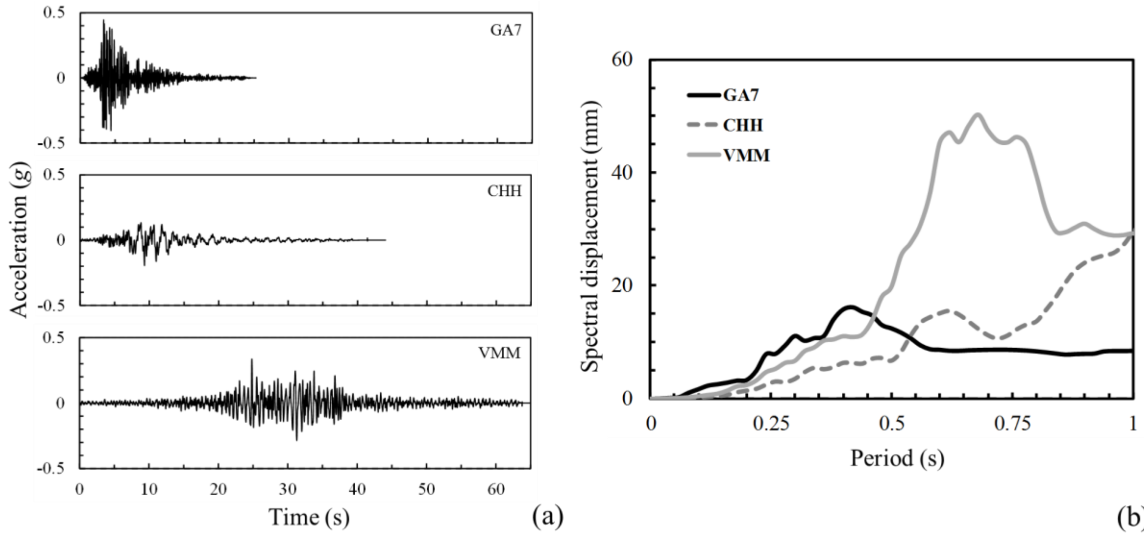

Fig. 6 – Input ground motions: (a) acceleration histories; (b) elastic displacement response spectra (ξ = 5%)

Table 1. Input motions characteristics

Record ID	Earthquake	Station	R (km)	PGA (g)	D_S (s)
GA7	Loma Prieta, CA 1989	Gilroy Array #7	24	0.45	7.2
CHH	Darfield, NZ 2010	Christchurch Hospital	42	0.20	12.8
VMM	Maule, Chile 2010	Viña del Mar Marga-Marga	290	0.33	20.4

Table 2. Experimental program (selected tests)

Series	Test ID	Specimen	Input motion
S1	S1T1	As-built	GA7
S2	S2T1	As-built/repaired	CHH
S2	S2T2	As-built/repaired	VMM
S3	S3T1	Retrofitted	CHH
S3	S3T2	Retrofitted	VMM

5. Fundamental period of the specimen and elastic spectral displacements

The fundamental period of the specimen (T_1), measured before each test, is presented in Table 3. In order to provide an estimation of the maximum response of the specimen, the elastic spectral displacements for each period are also shown in Table 3. It is noted that similar maximum displacements are predicted for tests S1T1 and S2T2, for example.

Table 3. Fundamental periods of vibration and spectral displacement

Test ID	Specimen	T_1 (s)	S_d (mm)
S1T1	As-built	0.24	8
S2T1	As-built/repaired	0.27	3
S2T2	As-built/repaired	0.33	9
S3T1	Retrofitted	0.32	5
S3T2	Retrofitted	0.35	10

6. Experimental results

In the following figures, the response of the specimen during the different tests is presented in terms of the histories of the inter-storey drift ratios (*dr*) of each level (dr_1, dr_2, and dr_3 for storeys 1, 2, and roof, respectively). Firstly, the response of the as-built and as-built/repaired specimens during three tests are examined. Secondly, the results of the retrofitted and the as-built/repaired specimens are compared.

6.1. As-built vs as-built/repaired specimens

Fig. 7 compares the results of the tests S1T1 and S2T1. As shown in this figure, during both tests the amplitude of *dr* remained close to or below 1% in the three levels (see Table 4), value associated with an elastic response in this case. The amplitude of the response remained approximately constant over the height during test S1T1, whereas it decreased from floor 1 to the roof during test S2T1. The strong part of the motion of the specimen during test S1T1 started at approximately 2.5 seconds and lasted for about 4 seconds only. During test S2T1 it started after 6 seconds, approximately, and lasted for about 10 seconds. The maximum values of dr_i obtained during each test ($dr_{i,max}$) are shown in Table 4.

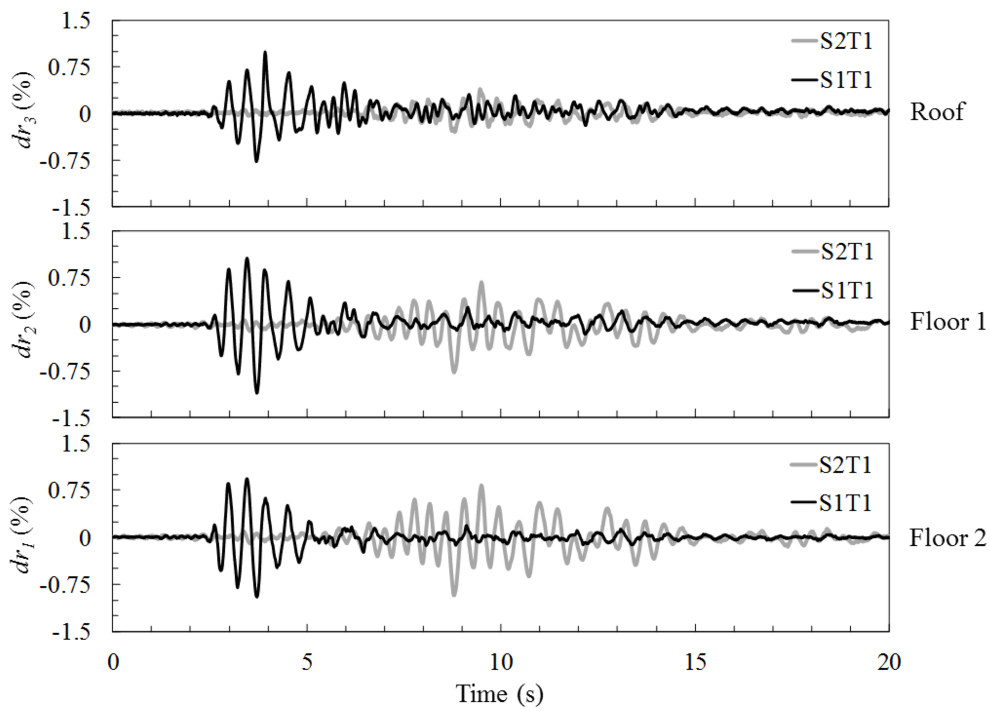

Fig.7 – Inter-storey drift ratios (*dr*) tests S1T1, S2T1.

Table 4. Maximum inter-storey drift ratios, *dr* (%), tests S1T1, S2T1 and S2T2

Level\Test	S1T1	S2T1	S2T2
Roof	0.99	0.40	0.90
2	1.10	0.69	2.60
1	0.93	0.92	3.82

Fig. 8 compares the results of the tests S2T2, S1T1 and S2T1. Fig. 8 reflects the large difference in the duration and magnitude of the *dr* histories obtained during test S2T2 and the other two tests. In this case, $dr_{1,max}$ reached 3.82%, a value that can be considered very close to a collapse limit state. The value of *dr* decreased over the height of the building, reaching 2.6% and 0.9% in floor 2 and roof, respectively (see Table 4). The strong part of the motion slowly started at about 10 seconds after the beginning of the test, and lasted for 30 seconds approximately.

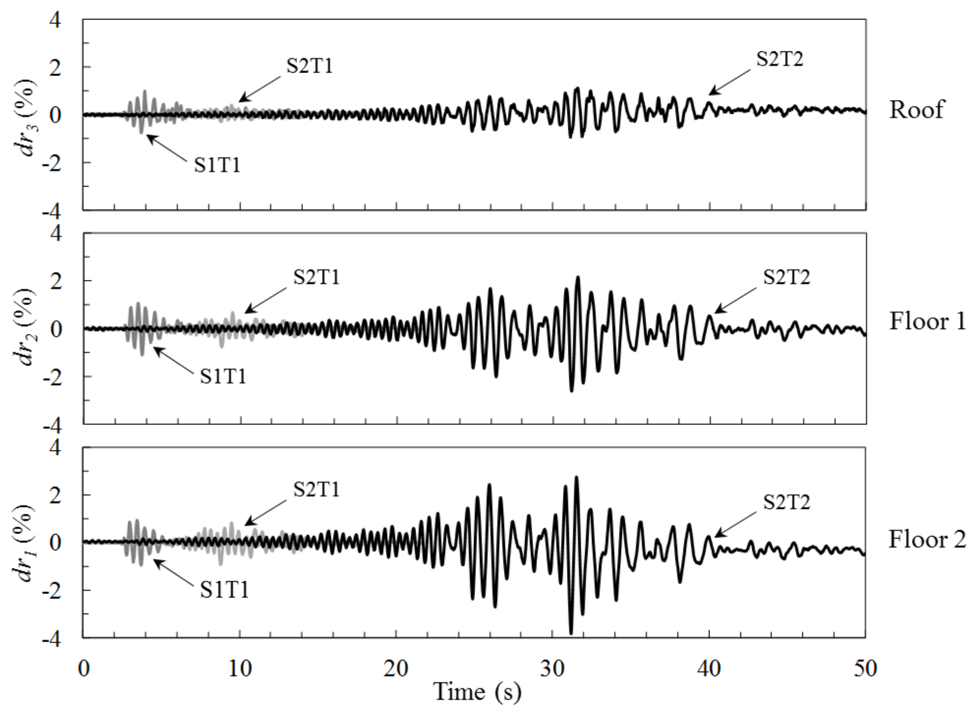

Fig. 8 – Inter-storey drift ratios (*dr*) tests S2T2, S1T1, S2T1.

No significant damage was observed in the specimen after tests S1T1 and S2T1. Only after S2T1, some fine cracks were observed to have developed in corner joints. During the test S2T2, on the other hand, extensive cracking and crushing of the concrete occurred in the joints and columns of corner and cruciform b-c joints, respectively. Crushing of the concrete in the interior columns was also observed. Some of that damage is illustrated in the pictures of Fig. 9. See [21] for details.

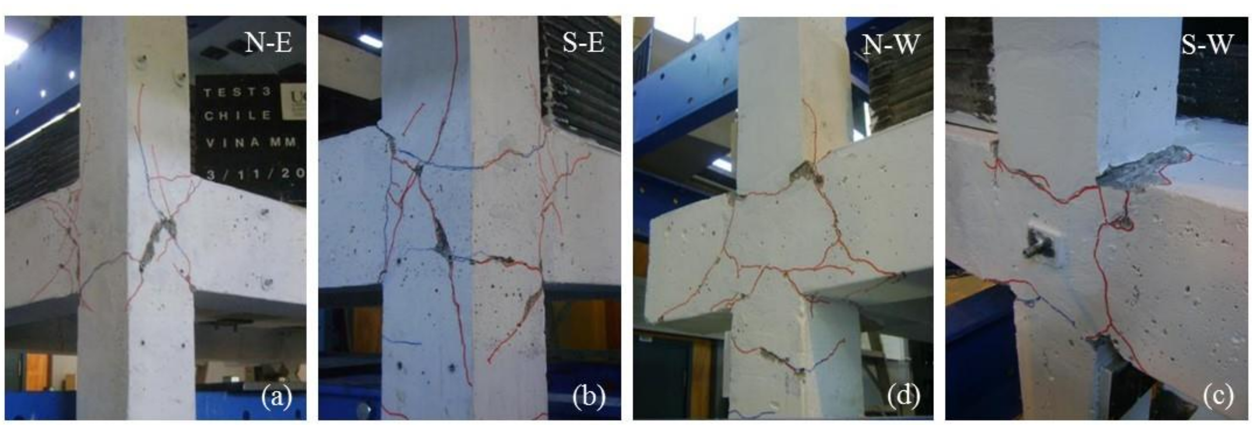

Fig. 9 – Damage in exterior b-c joints after test S2T2, level 1: (a) north-east corner; (b) south-east corner; (c) north-west cruciform; (d) south-west cruciform.

As shown in Fig. 9(a) and 9(b), both corner b-c joints suffered a shear-compression failure, forming a 'concrete wedge' mechanism, as previously found in b-c joint subassemblies with similar reinforcing detailing [6-8]. In this case, however, the damage was not as symmetric as in those specimens, but it was more intense in the exterior-bottom part of the joint. This is attributed to the presence of the floor slab and the transverse beam, together with the reduction of the axial load consistent with the slab acting in compression [21]. In cruciform b-c joints, on the other hand, the weakest link was the column, due to the greater confinement and larger joint effective width provided by the transverse beams on both sides. The analytical prediction of the hierarchy of strengths and sequence of events associated with each b-c joint type are presented in [21].

5.3. As-built/repaired vs retrofitted specimens

Fig. 10 and Fig. 11 compare the global response of the as-built/repaired and retrofitted specimens subjected to the records CHH and VMM, respectively. Fig. 10 shows that the *dr* histories obtained during tests S2T1 and S3T1 (CHH record) had similar shapes. The *dr* histories at all levels were almost identical during the initial and final parts of the response. They only differed in amplitude during the stronger part, indicating an apparently elastic response in both cases. During the strong part of the response, the amplitude of the recorded *dr* during test S3T1 was smaller than the one measured during the test S2T1, with dr_1 showing the largest reduction. The maximum values obtained during the test S3T1 are presented in Table 5, together with the reduction (or amplification) of the maximum *dr* obtained during test S2T1 (as-built/repaired counterpart).

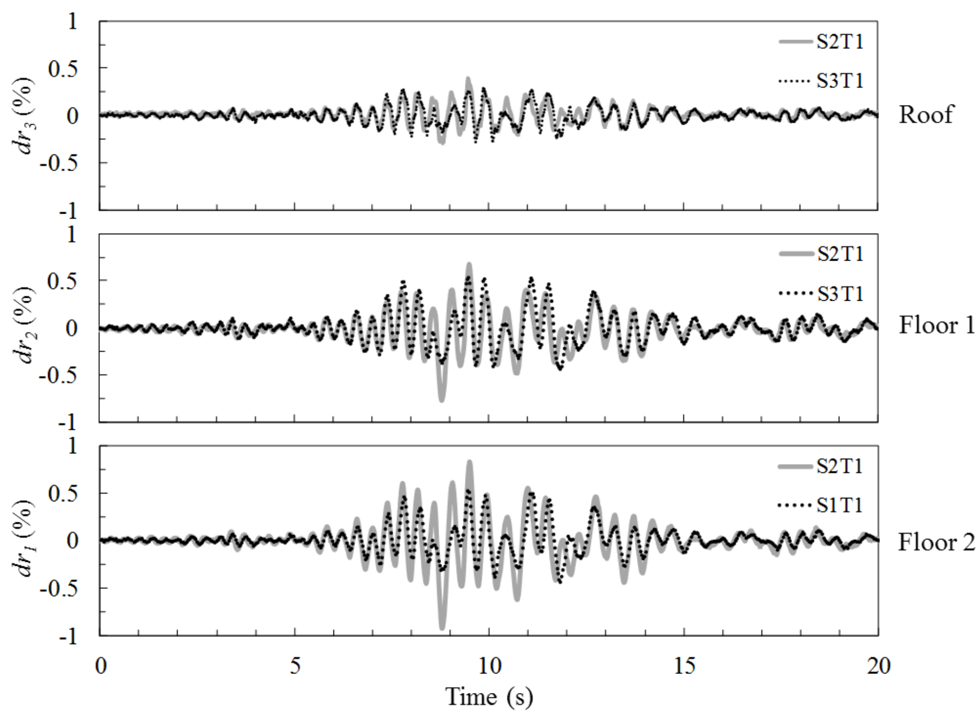

Fig. 10 – Inter-storey drift ratios (*dr*) tests S2T1, S3T1.

Table 5. Maximum *dr* (%) and reduction ratio (%) (R_1 and R_2) tests S3T1 and S3T2

Level\Test	S3T1	R_1	S3T2	R_2
Roof	0.30	25	0.98	-9
2	0.54	22	2.25	13
1	0.54	41	3.70	3

The graphs shown in Fig. 11 reflect very similar responses between the as-built/repaired and retrofitted specimens when subjected to the record VMM. At all the levels, the shape and amplitude of the *dr* histories obtained during these tests were very close to each other over the entire duration of the motion. There was no substantial reduction in the amplitude of dr_1 for the retrofitted specimen during the strong part of the motion, as for the CHH record. The maxima recorded at each level are presented in Table 5. Of particular interest is the amplitude of dr_1, which was reduced from 3.82% to 3.70% only (R_2 = 7%), which is still in the order of magnitude close to a collapse limit state. In addition, the vestiges of resonance in the response can be observed in Fig. 11 for both tests at approximately 20 seconds after the beginning of the motion.

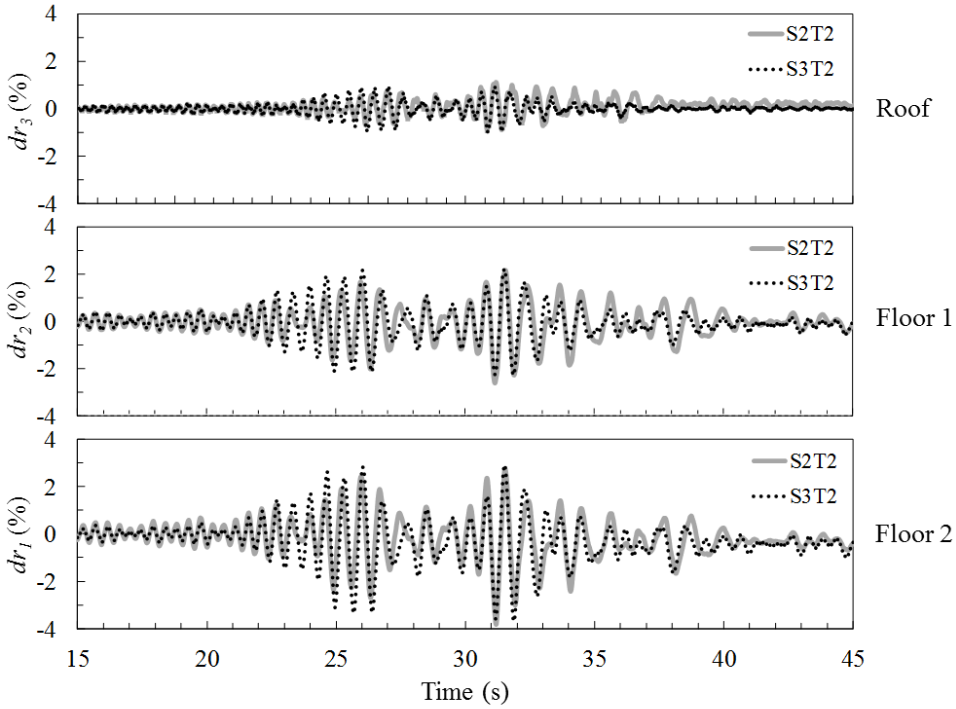

Fig. 11 – Measured inter-storey drift ratios (*dr*) tests S2T2, S3T2.

The damage experienced by the retrofitted specimen after test S3T2 was mainly concentrated in the beams of exterior b-c joints and the internal columns of the first level. Fig. 12(a) and 12(b) present the damage developed adjacent to corner b-c joints of the north and south facades, respectively. The pictures of those figures show how the fuse formed in the unretrofitted part of the beam, close to the GFRP laminates. In the south-east corner b-c joint (long span), two main cracks developed to a certain distance from the GFRP laminates. In the north-east corner (short span), the inelastic behaviour was concentrated in one main crack in the beam right at the intersection with the GFRP sheets. In the upper levels, a similar pattern developed in these b-c joints, with finer cracks [21]. In all the cases, there was no indication of cracks showing through the wrap at the joint.

Fig. 12 – Damage in exterior b-c joints after test S3T2, level 1: (a) north-east corner; (b) south-east corner; (c) north-west cruciform; (d) south-west cruciform.

The pictures of Fig. 12(c) and 12(d) show the damage observed in cruciform b-c joints of the first level. These pictures illustrate how the fuse also formed in the beam and not in the columns, with the exception of minor cracking in the columns [21]. In this case, the beam cracks developed mostly at the intersection with the spandrel and close to the beam GFRP laminates. The damage pattern in this case was the same in the b-c joints of the long and short spans. Crushing of the concrete was also observed in the interior columns [21].

6. Summary and Conclusions

The purpose of this investigation was to provide information about the dynamic response of a building typology with particularly brittle b-c joints, and to develop a new retrofit solution to upgrade its performance using cost effective non-invasive techniques. A series of shake-table tests was performed on a RC frame model structure with non-ductile detailing, as-built (with lap-splices), as-built/repaired (without lap-splices), and retrofitted with GFRP laminates plus weakening of the slab. The results showed that the as-built and as-built/repaired specimens experienced remarkably different responses, strongly dependant on the duration and frequency content of the input motions. During two tests with short duration input motions and PGA of 0.45g and 0.20g, respectively, the specimen responded mostly within the elastic range. During the test with the large duration record, with PGA 0.33g, the specimen suffered severe damage in exterior b-c joints and interior columns, as a result of an apparent resonant response of the specimen. The results also showed that the retrofit strategy achieved the main goal of relocating the damage from the joints into the beams in exterior b-c joints, under large inter-storey drift demands. As a consequence, the inelastic mechanism of the structure during the motion shifted from brittle to a more ductile and stable one. However, the retrofit strategy was not able to substantially diminish the amplitude of the response, particularly in terms of the first level inter-storey drift ratio. The tests confirmed the seismic vulnerability of the typology under investigation, regardless of the specimen not being highly affected during some of the tests. They also showed that the developed retrofit solution provides a tool that can be implemented in practice, but needs further investigation, ideally using full-scale shake-table tests.

7. Acknowledgements

This project was founded by the ‘Foundation for Research, Science and Technology’ *Tūāpapa Rangahau Pūtaiao*, New Zealand. Thanks to Dr. Weng Y. Kam, Dr. Umut Akguzel, Dr. Sahin Tasligedik, Mr. John Maley, Dr. Antonio Di Cesare, Mr. Domenico Nigro, Professor Patricio Bonelli, and the technical staff of the Structures Laboratory of the University of Canterbury for their help during the development of this research. Special thanks to Mr. Mosese Fifita for his great technical contribution. The support provided by BRANZ for writing this paper and the assistance of Dr. Patricia Shaw, Mr. Graeme Beattie and Dr. David Carradine is much appreciated.

8. References

[1] Hanson NW, Connor HW (1967): Seismic resistance of reinforced concrete beam-column joints. *Journal of the Structural Division*, **93** (5), 533-570.

[2] Aycardi LE, Mander JB, Reinhorn AM (1994): Seismic resistance of reinforced concrete frame structures designed only for gravity loads - experimental performance of subassemblages. *ACI Struct. J.*, **91** (5), 552-563.

[3] Beres A, Pessiki S, White R, Gergely P (1996): Implications of experiments on the seismic behaviour of gravity load designed RC beam-to-column connections. *Earthquake Spectra*, **12** (2), 185-198.

[4] Hakuto S, Park R, Tanaka H (2000): Seismic load tests on interior and exterior beam-column joints with substandard reinforcing details. *ACI Struct. J.*, **97** (1), 11-25.

[5] Li B, Wu Y, Pan TC (2002): Seismic behavior of non-seismically detailed interior beam-wide column joints. part i: experimental results and observed behavior. *ACI Struct. J.*, **99** (6), 791-802.

[6] Pampanin S, Calvi GM, Moratti M (2002): Seismic behavior of RC beam column joints designed for gravity loads. *12th European Conference on Earthquake Engineering*, London, England.

[7] Akguzel U, Pampanin S (2010): Effects of variation of axial load and bidirectional loading on seismic performance of GFRP retrofitted reinforced concrete exterior beam-column joints. *J. Comp. Constr.*, **14** (1), 94-104.

[8] Kam WY, Quintana Gallo P, Akguzel U, Pampanin S (2010): Influence of slab on the seismic response of substandard exterior reinforced concrete beam column joints. *9th US and 10th Canadian Conf. on Eq. Eng.*, Toronto, Canada.

[9] Calvi GM, Magenes G, Pampanin S (2002): Experimental test on a three storey R.C. frame designed for gravity loads only. *12th European Conference on Earthquake Engineering*, London, England.

[10] Di Ludovico M, Manfredi G, Mola E, Negro P, Prota A (2008): Seismic behavior of a full-scale rc structure retrofitted using GFRP laminates. *J. of Struct. Eng.*, **134** (5), 810-821.

[11] Ghannoum WM, Moehle JP (2012): Shake-table tests of a concrete frame sustaining column axial failures. *ACI Struct. J.*, **109** (3), 393-402.

[12] Yavari S, Elwood KJ, Wu CL, Lin SH, Hwang SJ, Moehle JP (2013): Shaking table tests on reinforced concrete frames without seismic detailing. *ACI Struct. J.*, **110** (6), 1001-1011.

[13] Bracci J, Reinhorn A, Mander J (1995): Seismic resistance of reinforced concrete frame structures designed for gravity loads: performance of structural system. *ACI Struct. J.*, **92** (5), 597-609.

[14] Bracci J, Reinhorn A, Mander J (1995): Seismic retrofit of reinforced concrete buildings designed for gravity loads: performance of structural model. *ACI Struct. J.*, **92** (6), 711-723.

[15] Chaudat T, Pilakoutas K., Papastergiou P, Ciupala MA (2006): Shaking table test son reinforced concrete retrofitted frame with fiberglass reinforced plastic (FRP). European Conf. on Eq. Eng. and Seismology, Geneva, Switzerland.

[16] Garcia R, Hajirasouliha I, Guadagnini M, Helal Y, Jemaa Y, Pilakoutas K, Mongabure P, Chrysostomou C, Kyriakydes N, Ilki A, Budescu M, Tarantu N, Ciupala MA, Torres L, Saiidi M (2014): Full-scale shaking table tests on a substandard RC building repaired and strengthened with post-tensioned metal straps. *J. Eq. Eng.*, **18** (2), 187-213.

[17] Garcia R, Pilakoutas K, Hajirasouliha I, Guadagnini M, Kyriakydes N, Ciupala MA (2015): Seismic retrofitting of RC buildings using CFRP and post-tensioned metal straps: shake table tests. *Bull. Eq. Eng.*, **DOI** 10.1007/s10518-015-9800-8.

[18] Sharma A, Reddy GR, Eligehausen R, Genesio G, Pampanin S (2014): Seismic response of reinforced concrete frames with haunch retrofit solution. *ACI Struct. J.*, **111** (3), 673-684.

[19] Pampanin S, Christopoulos C, Chen TH (2006): Development and validation of a Metallic Haunch seismic retrofit system for existing under-designed RC frame buildings. *Eq. Eng. Struct. Dyn.*, **35** (14), 1739-1766.

[20] Marriott DJ, Pampanin S, Bull DK, Palermo A (2007): Improving the seismic performance of existing reinforced concrete buildings using advanced rocking wall solutions. *NZSEE Annual Conference*, Palmerston North, New Zealand.

[21] Quintana Gallo P (2014): *The Nonlinear Dynamics Involved in the Seismic Assessment and Retrofit of RC Buildings*, PhD Thesis, Department of Civil and Natural Resources Engineering, University of Canterbury, Christchurch, New Zealand.

[22] Morcarz P, Krawinkler H (1981): *Theory and Application of Experimental Model Analysis in Earthquake Engineering*. Report No.50, John Blume Earthquake Engineering Center, Department of Civil and Environmental Engineering, Stanford University, Stanford, CA.

[23] Quintana Gallo P, Pampanin S, Carr AJ, Bonelli P (2010): Shake table tests of under-designed RC frames for the seismic retrofit of buildings – design and similitude requirements of the benchmark specimen. *NZSEE Annual Conference*, Auckland, New Zealand.

[24] Pampanin S (2006): Controversial aspects in seismic assessment and retrofit of structures in modern times: understanding and implementing lessons from ancient heritage. *Bulletin of the NZSEE*, **39** (2), 120-133.

[25] Pampanin S, Bolognini D, Pavese A (2007): Performance-based seismic retrofit strategy for existing reinforced concrete frame systems using fiber-reinforced polymer composites. *J. Comp. Constr.*, **11** (2), 211-226.

[26] Akguzel U, Pampanin S (2012): Assessment and design procedure for the seismic retrofit of reinforced concrete beam-column joints using FRP composite materials. *J. Comp. Constr.*, **16** (1), 21-34.

[27] Trifunac MD, Brady AG (1975): A study on the duration of strong earthquake ground motion. *Bull. Seism. Soc. Am.*, **65** (3), 581-626.